

# A Flexible and Parsimonious Modelling Strategy for Clustered Data Analysis

Tao Huang<sup>1</sup>, Youquan Pei<sup>2</sup>, Jinhong You<sup>1</sup>, and Wenyang Zhang<sup>\*3</sup>

<sup>1</sup>School of Statistics and Management, Shanghai University of Finance and Economics, CN

<sup>2</sup>School of Economics, Shandong University, CN

<sup>3</sup>Department of Mathematics, University of York, UK

## Abstract

Statistical modelling strategy is the key for success in data analysis. The trade-off between flexibility and parsimony plays a vital role in statistical modelling. In clustered data analysis, in order to account for the heterogeneity between the clusters, certain flexibility is necessary in the modelling, yet parsimony is also needed to guard against the complexity and account for the homogeneity among the clusters. In this paper, we propose a flexible and parsimonious modelling strategy for clustered data analysis. The strategy strikes a nice balance between flexibility and parsimony, and accounts for both heterogeneity and homogeneity well among the clusters, which often come with strong practical meanings. In fact, its usefulness has gone beyond clustered data analysis, it also sheds promising lights on transfer learning. An estimation procedure is developed for the unknowns in the resulting model, and asymptotic properties of the estimators are established. Intensive simulation studies are conducted to demonstrate how well the proposed methods work, and a real data analysis is also presented to illustrate how to apply the modelling strategy and associated estimation procedure to answer some real problems arising from real life.

*Keywords:* Clustered data analysis, structure identification, semiparametric models.

---

\*The corresponding author, Email: [wenyang.zhang@york.ac.uk](mailto:wenyang.zhang@york.ac.uk)

# 1 Introduction

The data, which stimulates this paper, come from 29 provinces (for the sake of convenience, municipalities are also called provinces in this paper) in China. It includes the daily number of Covid-19 infected cases, of people from Wuhan to a province, of cured cases, and maximum daily temperature in the province from 9 January 2020 to 25 March 2020, it also includes the population size of the province. This dataset is a typical clustered dataset with each individual of length 77. We focus on the log ratio,  $y_{i,t}$ , of the cumulative number of infected cases in the  $i$ th province at time point  $t$  to that at time point  $t - 1$ . We call  $y_{i,t}$  the infection ratio at time point  $t$  in the  $i$ th province. As cured cases may not have much effect on infection ratio, we exclude it from our analysis and focus on maximum daily temperature in a province, denoted by  $x_{i,t,1}$ , and the number of people from Wuhan to the province, denoted by  $x_{i,t,2}$ . What we are interested in are: how maximum daily temperature in a province and the number of people from Wuhan to the province affect the infection ratio in the province? Whether their impacts change over time? If they do, what are the dynamic patterns of the impacts? Whether the impacts vary over different provinces? Are there provinces sharing the same impacts? If there are, which provinces share the same impacts?

The varying coefficient models are a powerful tool to explore nonlinear dynamic patterns of impacts of covariates. There is much literature about the varying coefficient models (Zhang and Lee, 2000; Zhang et al., 2002; Liu et al., 2014; Cheng and Fan, 2016; Cheng et al., 2016; Chu et al., 2020), and its application in the analysis of time series data (Li and Li, 2008, 2011; Wang and Xia, 2015; Lei et al., 2016) and of clustered data (Li et al., 2015, 2017; Zhong et al., 2019; Xu et al., 2020; Feng et al., 2021). We start with the standard

varying coefficient models, which leads to

$$y_{i,t} = b_i + a_{i,1}(u_{i,t})x_{i,t,1} + a_{i,2}(u_{i,t})x_{i,t,2} + \epsilon_{i,t}, \quad u_{i,t} = t/77. \quad (1.1)$$

Whilst the dynamic patterns of the impacts of  $x_{i,t,1}$  and  $x_{i,t,2}$  have been reflected and formulated by  $a_{i,1}(\cdot)$  and  $a_{i,2}(\cdot)$ , this modelling assumes the contribution of covariates to response is linear, functional coefficients though. This may not be realistic, indeed, in Section 5, we will see this assumption is not valid, and the contribution of covariates is in fact through transformed covariates. Furthermore, this modelling has not taken into account the effects of previous infection ratios. To overcome these problems takes us to the following model

$$\begin{aligned} y_{i,t} = & b(u_{i,t}) + \sum_{j=1}^p a_{i,j}(u_{i,t})g_{i,j}(y_{i,t-j}) + a_{i,p+1}(u_{i,t})g_{i,p+1}(x_{i,t,1}) \\ & + a_{i,p+2}(u_{i,t})g_{i,p+2}(x_{i,t,2}) + \eta_i + \epsilon_{i,t}, \end{aligned} \quad (1.2)$$

where  $b(\cdot)$ ,  $a_{i,k}(\cdot)$ s and  $g_{i,k}(\cdot)$ s are unknown functions, and  $\eta_i$ s are random effects. To answer the question that which provinces share the same impacts, we assume some of  $a_{i,k}(\cdot)$ s are the same, and some of  $g_{i,k}(\cdot)$ s are the same. We don't assume which  $a_{i,k}(\cdot)$ s or  $g_{i,k}(\cdot)$ s are the same, and let data identify. Putting this modelling idea in a more formal and generic form leads to the following class of semiparametric models for clustered data analysis.

Rather than confining us to the Covid-19 dataset, we assume  $y_{i,t}$  is the observation of the response variable of the  $i$ th individual at time point  $t$ ,  $(u_{i,t}, \mathbf{X}_{i,t})$  the vector of the corresponding covariates, where  $\mathbf{X}_{i,t} = (x_{i,t,1}, \dots, x_{i,t,q})^\tau$  is of dimension  $q$ ,  $u_{i,t}$  is a scalar.

We assume

$$y_{i,t} = b(u_{i,t}) + \sum_{j=1}^p a_{i,j}(u_{i,t})g_{i,j}(y_{i,t-j}) + \sum_{l=1}^q a_{i,p+l}(u_{i,t})g_{i,p+l}(x_{i,t,l}) + \eta_i + \epsilon_{i,t} \quad (1.3)$$

when  $t = p + 1, \dots, T_i^*$ ,  $i = 1, \dots, n$ .  $x_{i,t,l}$  is the  $l$ th component of  $\mathbf{X}_{i,t}$ ,  $\eta_i$  a random effect with mean 0 and variance  $\sigma_\eta^2$ .  $\epsilon_{i,t}$  is a random error with mean 0, variance  $\sigma^2$ .  $b(\cdot)$ ,  $a_{i,j}(\cdot)$ s, and  $g_{i,j}(\cdot)$ s are all unknown functions to be estimated.

Apparently, (1.3) is not identifiable. To make it identifiable, we assume

$$E\{a_{i,j}(u_{i,t})\} = 1, E\{g_{i,j}(y_{i,t-j})\} = 0, E\{a_{i,p+l}(u_{i,t})\} = 1, E\{g_{i,p+l}(x_{i,t,l})\} = 0, \quad (1.4)$$

for  $i = 1, \dots, n$ ,  $j = 1, \dots, p$  and  $l = 1, \dots, q$ .

We also assume

$$a_{i,j}(\cdot) = \begin{cases} \alpha_1(\cdot) & \text{if } (i,j) \in \mathcal{D}_1 \\ \vdots & \vdots \\ \alpha_H(\cdot), & \text{if } (i,j) \in \mathcal{D}_H \end{cases} \quad g_{i,j}(\cdot) = \begin{cases} \beta_1(\cdot) & \text{if } (i,j) \in \Delta_1 \\ \vdots & \vdots \\ \beta_m(\cdot) & \text{if } (i,j) \in \Delta_m \end{cases} \quad (1.5)$$

where  $\alpha_k(\cdot)$ 's and  $\beta_k(\cdot)$ 's are unknown functions to be estimated, and  $\{\mathcal{D}_1, \dots, \mathcal{D}_H\}$  is an unknown partition of

$$\{(i,j) : i = 1, \dots, n; j = 1, \dots, p+q\},$$

and so is  $\{\Delta_1, \dots, \Delta_m\}$ . Except for the practical implication mentioned before, condition (1.5) also serves, in statistical modelling, to make model (1.3) more parsimonious.

---

\*We allow the time series length  $T_i$  to be heterogeneous across  $i$ , which corresponding to unbalanced clustered data.

Model (1.3) under conditions (1.4) and (1.5) is the model we are going to address in this paper.

We would like to stress that (1.3) is a large class of semiparametric models, which include nonparametric autoregressive models (Huang and Yang, 2004; Sun et al., 2014; Lei et al., 2016; Sun, 2016; Kalli and Griffin, 2018), varying coefficient models and additive models (Wood et al., 2015; Chen et al., 2018; Sang et al., 2020).

Condition (1.5) can also be viewed as a latent structure. Latent structure identification is a very useful statistical modelling idea and has been widely used in the analysis of cross sectional data (Ke et al., 2015; Fan et al., 2017; Ren et al., 2019; Wu et al., 2020; Fan et al., 2022; Yuan et al., 2022), of time series data (Bahadori et al., 2015; Ke et al., 2022) and of clustered data (Bonhomme and Manresa, 2015; Ke et al., 2016; Su et al., 2016; Chen, 2019; Li et al., 2019; Xu et al., 2020; Lian et al., 2021; Xiao et al., 2021; Guo and Li, 2022; Pei et al., 2022; Zhu et al., 2022).

In this paper, we make contributions on three fronts. Firstly, we propose a flexible and parsimonious modelling strategy for clustered data analysis, which results in a large class of semiparametric models, embedded with latent structures. It takes dynamic nonparametric models, varying coefficient models and additive models as its special cases. Secondly, we develop a procedure, which is easy to implement by the proposed computational algorithm, to identify the latent structures and estimate cluster-specific functions. Thirdly, we demonstrate the advantage of the proposed methodology by asymptotic theory and empirical analysis.

The rest of the paper is organised as follows. We describe our estimation procedure and the computational algorithm to implement it in Section 2. In Section 3, we present the asymptotic properties of the estimators resulted from either the proposed estimation,

overfitting, or underfitting. Overfitting and underfitting will be defined at the beginning of Section 3. Intensive simulation studies are conducted in Section 4 to demonstrate how well the proposed estimation procedure works and the risk of ignoring homogeneity or heterogeneity among the individuals in a clustered dataset. In Section 5, we apply the proposed models and estimation procedure to the Covid-19 dataset, and explore how maximum daily temperature in a province and the number of people from Wuhan to the province affect the infection ratio in the province. We will identify which provinces in China share the same impacts, and find out the dynamic patterns of the impacts. Throughout this paper, a superscript  $\tau$  indicates the transpose of a vector or a matrix.  $\xrightarrow{D}$  indicates convergence in a distribution.

## 2 Estimation procedure

### 2.1 Estimation method

The proposed estimation procedure consists of three stages: initial estimation, structure identification, and final estimation. For the sake of convenience in the structure identification in our estimation procedure, without loss of generality, we assume the range of each covariate involved in (1.3) and of  $y_{i,t}$  is  $[0, 1]$ .

We apply B-spline decomposition, with knots being equally placed, to deal with the unknown functions in (1.3). The number of knots used for the final estimation is larger than that for the initial estimation due to the common structure identified being used, therefore, the basis functions for the final estimation are different to that for the initial estimation. Specifically, we use  $B_\ell(\cdot)$ ,  $\ell = 1, \dots, K$ , to denote the B-spline basis functions

used for the final estimation,  $B_\ell^{(0)}(\cdot)$ ,  $\ell = 1, \dots, K_0$ , for the initial estimation. Let

$$\begin{aligned}\bar{B}_{i,u,\ell} &= \frac{1}{T_i} \sum_{t=1}^{T_i} B_\ell(u_{i,t}), & \bar{B}_{i,y,j,\ell} &= \frac{1}{T_i - j} \sum_{t=1+j}^{T_i} B_\ell(y_{i,t-j}), \\ \bar{B}_{i,x,l,\ell} &= \frac{1}{T_i} \sum_{t=1}^{T_i} B_\ell(x_{i,t,l}). & \mathbf{B}_{i,0,t} &= (B_1(u_{i,t}), \dots, B_K(u_{i,t}))^\tau, \\ \mathbf{B}_{i,u,t} &= (B_1(u_{i,t}) - \bar{B}_{i,u,1}, \dots, B_K(u_{i,t}) - \bar{B}_{i,u,K})^\tau, \\ \mathbf{B}_{i,y,j,t} &= (B_1(y_{i,t-j}) - \bar{B}_{i,y,j,1}, \dots, B_K(y_{i,t-j}) - \bar{B}_{i,y,j,K})^\tau, \\ \mathbf{B}_{i,x,l,t} &= (B_1(x_{i,t,l}) - \bar{B}_{i,x,l,1}, \dots, B_K(x_{i,t,l}) - \bar{B}_{i,x,l,K})^\tau.\end{aligned}$$

Under condition (1.4), in the final estimation,

$$\begin{aligned}b(u_{i,t}) &\approx \mathbf{B}_{i,0,t}^\tau \mathbf{b}, & a_{i,j}(u_{i,t}) &\approx 1 + \mathbf{B}_{i,u,t}^\tau \mathbf{a}_{i,j}, & a_{i,p+l}(u_{i,t}) &\approx 1 + \mathbf{B}_{i,u,t}^\tau \mathbf{a}_{i,p+l} \\ g_{i,j}(y_{i,t-j}) &\approx \mathbf{B}_{i,y,j,t}^\tau \mathbf{g}_{i,j}, & g_{i,p+l}(x_{i,t,l}) &\approx \mathbf{B}_{i,x,l,t}^\tau \mathbf{g}_{i,p+l},\end{aligned}\tag{2.1}$$

where  $i = 1, \dots, n$ ,  $j = 1, \dots, p$  and  $l = 1, \dots, q$ . We use superscript (0) to denote the counterpart of this notation in the initial estimation, e.g.  $\mathbf{B}_{i,0,t}^{(0)}$  is the counterpart of  $\mathbf{B}_{i,0,t}$ .

In the initial estimation,

$$\begin{aligned}b(u_{i,t}) &\approx \mathbf{B}_{i,0,t}^{(0)\tau} \mathbf{b}^{(0)}, & a_{i,j}(u_{i,t}) &\approx 1 + \mathbf{B}_{i,u,t}^{(0)\tau} \mathbf{a}_{i,j}^{(0)}, & a_{i,p+l}(u_{i,t}) &\approx 1 + \mathbf{B}_{i,u,t}^{(0)\tau} \mathbf{a}_{i,p+l}^{(0)} \\ g_{i,j}(y_{i,t-j}) &\approx \mathbf{B}_{i,y,j,t}^{(0)\tau} \mathbf{g}_{i,j}^{(0)}, & g_{i,p+l}(x_{i,t,l}) &\approx \mathbf{B}_{i,x,l,t}^{(0)\tau} \mathbf{g}_{i,p+l}^{(0)}.\end{aligned}\tag{2.2}$$

### 2.1.1 Initial estimation

We treat all unknown functions in (1.3) as different functions to estimate. Applying the least squares estimation and the approximations in (2.2), we have the following objective

function

$$\sum_{t=p+1}^{T_i} \left\{ y_{i,t} - \mathbf{B}_{i,0,t}^{(0)\tau} \mathbf{b}_i^{(0)} - \sum_{j=1}^p \left( 1 + \mathbf{B}_{i,u,t}^{(0)\tau} \mathbf{a}_{i,j}^{(0)} \right) \mathbf{B}_{i,y,j,t}^{(0)\tau} \mathbf{g}_{i,j}^{(0)} - \sum_{l=1}^q \left( 1 + \mathbf{B}_{i,u,t}^{(0)\tau} \mathbf{a}_{i,p+l}^{(0)} \right) \mathbf{B}_{i,x,l,t}^{(0)\tau} \mathbf{g}_{i,p+l}^{(0)} \right\}^2. \quad (2.3)$$

We minimise (2.3) with respect to  $\mathbf{b}_i^{(0)}$ ,  $\mathbf{a}_{i,j}^{(0)}$ s,  $\mathbf{g}_{i,j}^{(0)}$ s,  $\mathbf{a}_{i,p+l}^{(0)}$ s and  $\mathbf{g}_{i,p+l}^{(0)}$ s, and denote the minimisers as  $\tilde{\mathbf{b}}_i^{(0)}$ ,  $\tilde{\mathbf{a}}_{i,j}^{(0)}$ s,  $\tilde{\mathbf{g}}_{i,j}^{(0)}$ s,  $\tilde{\mathbf{a}}_{i,p+l}^{(0)}$ s and  $\tilde{\mathbf{g}}_{i,p+l}^{(0)}$ s. We use

$$\tilde{b}_i(\cdot) = \left( B_1^{(0)}(\cdot), \dots, B_{K_0}^{(0)}(\cdot) \right)^\tau \tilde{\mathbf{b}}_i^{(0)},$$

$$\tilde{a}_{i,j}(\cdot) = 1 + \left( B_1^{(0)}(\cdot) - \bar{B}_{i,u,1}^{(0)}, \dots, B_{K_0}^{(0)}(\cdot) - \bar{B}_{i,u,K_0}^{(0)} \right)^\tau \tilde{\mathbf{a}}_{i,j}^{(0)},$$

$$\tilde{g}_{i,j}(\cdot) = \left( B_1^{(0)}(\cdot) - \bar{B}_{i,y,j,1}^{(0)}, \dots, B_{K_0}^{(0)}(\cdot) - \bar{B}_{i,y,j,K_0}^{(0)} \right)^\tau \tilde{\mathbf{g}}_{i,j}^{(0)},$$

$$\tilde{a}_{i,p+l}(\cdot) = 1 + \left( B_1^{(0)}(\cdot) - \bar{B}_{i,u,1}^{(0)}, \dots, B_{K_0}^{(0)}(\cdot) - \bar{B}_{i,u,K_0}^{(0)} \right)^\tau \tilde{\mathbf{a}}_{i,p+l}^{(0)},$$

$$\tilde{g}_{i,p+l}(\cdot) = \left( B_1^{(0)}(\cdot) - \bar{B}_{i,x,l,1}^{(0)}, \dots, B_{K_0}^{(0)}(\cdot) - \bar{B}_{i,x,l,K_0}^{(0)} \right)^\tau \tilde{\mathbf{g}}_{i,p+l}^{(0)},$$

$i = 1, \dots, n$ ,  $j = 1, \dots, p$ ,  $l = 1, \dots, q$ , as the initial estimators of  $b(\cdot) + \eta_i$ ,  $a_{i,j}(\cdot)$ ,  $g_{i,j}(\cdot)$ ,  $a_{i,p+l}(\cdot)$ , and  $g_{i,p+l}(\cdot)$ , respectively.

### 2.1.2 Structure identification

Throughout this paper, for any function  $f(\cdot)$  on  $[0, 1]$ , define  $\|f\|_2 = \int_0^1 f^2(v) dv$ . We first estimate the partition  $\{\Delta_1, \dots, \Delta_m\}$  by using the idea in [Vogt and Linton \(2017\)](#) and [Pei et al. \(2022\)](#). We start with  $\tilde{g}_{1,1}(\cdot)$ , and compute

$$\delta_{ij} = \frac{1}{\|\tilde{g}_{1,1}\|_2} \int_0^1 \{\tilde{g}_{1,1}(v) - \tilde{g}_{i,j}(v)\}^2 dv, \quad (i, j) \in \mathcal{S},$$



where  $\mathcal{S} = \{(i, j) : i = 1, \dots, n; j = 1, \dots, p + q\}$ . Let  $\hat{\Delta}_1$  be the set of all  $(i, j)$ s that satisfy  $\delta_{ij} < \mathcal{C}$ , where  $\mathcal{C}$  is a given threshold. In practice, it can be selected by cross-validation.

We select an element, say  $(i_0, j_0)$ , from  $\mathcal{S} - \hat{\Delta}_1$ , and compute

$$\delta_{ij} = \frac{1}{\|\tilde{g}_{i_0, j_0}\|_2} \int_0^1 \{\tilde{g}_{i_0, j_0}(v) - \tilde{g}_{i, j}(v)\}^2 dv, \quad (i, j) \in \mathcal{S} - \hat{\Delta}_1.$$

Let  $\hat{\Delta}_2$  be the set of all  $(i, j)$ s in  $\mathcal{S} - \hat{\Delta}_1$  that satisfy  $\delta_{ij} < \mathcal{C}$ . Continuously doing so, we get  $\{\hat{\Delta}_1, \dots, \hat{\Delta}_{\hat{m}}\}$  and use it to estimate  $\{\Delta_1, \dots, \Delta_m\}$ . Using exactly the same approach, we can get the estimator  $\{\hat{\mathcal{D}}_1, \dots, \hat{\mathcal{D}}_{\hat{H}}\}$  of  $\{\mathcal{D}_1, \dots, \mathcal{D}_H\}$ .

### 2.1.3 Final estimation

Let  $\mathbf{M}_i = (\mathcal{F}_{i, p+1}, \dots, \mathcal{F}_{i, T_i})^\tau$  and  $\mathcal{F}_{i, t}$  be

$$\mathbf{B}_{i, 0, t}^\tau \mathbf{b} + \sum_{j=1}^p (1 + \mathbf{B}_{i, u, t}^\tau \mathbf{a}_{i, j}) \mathbf{B}_{i, y, j, t}^\tau \mathbf{g}_{i, j} + \sum_{l=1}^q (1 + \mathbf{B}_{i, u, t}^\tau \mathbf{a}_{i, p+l}) \mathbf{B}_{i, x, l, t}^\tau \mathbf{g}_{i, p+l}$$

with  $\mathbf{a}_{\iota, \ell}$ ,  $\iota = 1, \dots, n$ ,  $\ell = 1, \dots, p + q$ , being replaced by  $\boldsymbol{\alpha}_k$  if  $(\iota, \ell) \in \hat{\mathcal{D}}_k$ ,  $\mathbf{g}_{\iota, \ell}$ ,  $\iota = 1, \dots, n$ ,  $\ell = 1, \dots, p + q$ , being replaced by  $\boldsymbol{\beta}_k$  if  $(\iota, \ell) \in \hat{\Delta}_k$ .

To take the within cluster correlation into account in the final estimation, we have to get the estimators of  $\sigma_\eta^2$  and  $\sigma^2$  first. We estimate  $\sigma_\eta^2$  and  $\sigma^2$  based on the residuals of working independence fitting. Specifically, we first minimise

$$\sum_{i=1}^n (\mathbf{Y}_i - \mathbf{M}_i)^\tau (\mathbf{Y}_i - \mathbf{M}_i)$$

with respect to  $(\mathbf{b}, \boldsymbol{\alpha}_1, \dots, \boldsymbol{\alpha}_{\hat{H}}, \boldsymbol{\beta}_1, \dots, \boldsymbol{\beta}_{\hat{m}})$ , and denote the minimiser by

$$(\tilde{\mathbf{b}}, \tilde{\boldsymbol{\alpha}}_1, \dots, \tilde{\boldsymbol{\alpha}}_{\hat{H}}, \tilde{\boldsymbol{\beta}}_1, \dots, \tilde{\boldsymbol{\beta}}_{\hat{m}}).$$

Let  $\tilde{\mathbf{M}}_i$  be  $\mathbf{M}_i$  with  $\mathbf{b}$ ,  $\boldsymbol{\alpha}_{k_s}$  and  $\boldsymbol{\beta}_{k_s}$  being replaced by  $\tilde{\mathbf{b}}$ ,  $\tilde{\boldsymbol{\alpha}}_{k_s}$  and  $\tilde{\boldsymbol{\beta}}_{k_s}$ . We then have the following objective function:

$$\sum_{i=1}^n \left\| (\mathbf{Y}_i - \tilde{\mathbf{M}}_i)(\mathbf{Y}_i - \tilde{\mathbf{M}}_i)^\tau - \sigma^2 I_{T_i} - \sigma_\eta^2 \mathbf{1}_{T_i} \mathbf{1}_{T_i}^\tau \right\|_2 \quad (2.4)$$

Applying the weighted least squares estimation, by simple calculation, we have the objective function:

$$\begin{aligned} & L(\mathbf{b}, \boldsymbol{\alpha}_1, \dots, \boldsymbol{\alpha}_{\hat{H}}, \boldsymbol{\beta}_1, \dots, \boldsymbol{\beta}_{\hat{m}}) \\ &= \sum_{i=1}^n (\mathbf{Y}_i - \mathbf{M}_i)^\tau \left( I_{T_i} - \frac{\hat{\sigma}_\eta^2}{T_i \hat{\sigma}_\eta^2 + \hat{\sigma}^2} \mathbf{1}_{T_i} \mathbf{1}_{T_i}^\tau \right) (\mathbf{Y}_i - \mathbf{M}_i) \end{aligned} \quad (2.5)$$

where  $\mathbf{Y}_i = (y_{i,p+1}, \dots, y_{i,T_i})^\tau$ .

We minimise (2.5) with respect to  $(\mathbf{b}, \boldsymbol{\alpha}_1, \dots, \boldsymbol{\alpha}_{\hat{H}}, \boldsymbol{\beta}_1, \dots, \boldsymbol{\beta}_{\hat{m}})$ , and denote the minimiser by

$$(\hat{\mathbf{b}}, \hat{\boldsymbol{\alpha}}_1, \dots, \hat{\boldsymbol{\alpha}}_{\hat{H}}, \hat{\boldsymbol{\beta}}_1, \dots, \hat{\boldsymbol{\beta}}_{\hat{m}}).$$

The final estimators of  $b(\cdot)$ ,  $a_{i,j}(\cdot)$ ,  $g_{i,j}(\cdot)$ ,  $a_{i,p+l}(\cdot)$  and  $g_{i,p+l}(\cdot)$  are

$$\hat{b}(\cdot) = (B_1(\cdot), \dots, B_K(\cdot))^\tau \hat{\mathbf{b}},$$

$$\hat{a}_{i,j}(\cdot) = 1 + (B_1(\cdot) - \bar{B}_{i,u,1}, \dots, B_K(\cdot) - \bar{B}_{i,u,K})^\tau \hat{\boldsymbol{\alpha}}_k, \quad \text{if } (i, j) \in \hat{\mathcal{D}}_k,$$

$$\hat{g}_{i,j}(\cdot) = (B_1(\cdot) - \bar{B}_{i,y,j,1}, \dots, B_K(\cdot) - \bar{B}_{i,y,j,K})^\tau \hat{\boldsymbol{\beta}}_k, \quad \text{if } (i, j) \in \hat{\Delta}_k,$$

$$\hat{a}_{i,p+l}(\cdot) = 1 + (B_1(\cdot) - \bar{B}_{i,u,1}, \dots, B_K(\cdot) - \bar{B}_{i,u,K})^\tau \hat{\boldsymbol{\alpha}}_k, \quad \text{if } (i, p+l) \in \hat{\mathcal{D}}_k,$$

$$\hat{g}_{i,p+l}(\cdot) = (B_1(\cdot) - \bar{B}_{i,x,l,1}, \dots, B_K(\cdot) - \bar{B}_{i,x,l,K})^\tau \hat{\boldsymbol{\beta}}_k, \quad \text{if } (i, p+l) \in \hat{\Delta}_k.$$

## 2.2 Computational algorithm

The main hurdle in the implementation of the proposed estimation method is the minimisation of (2.3) and (2.5). Because neither of them has a minimiser with closed form, we are going to minimise them by an iterative approach.

Applying the three-step spline estimation method proposed in Hu et al. (2019), we can easily get the initial values for  $\mathbf{g}_{i,j}^{(0)}$ 's and  $\mathbf{g}_{i,p+l}^{(0)}$ 's in (2.3). Replacing  $\mathbf{g}_{i,j}^{(0)}$ 's and  $\mathbf{g}_{i,p+l}^{(0)}$ 's in (2.3) by their initial values and minimising (2.3) with respect to  $\mathbf{b}_i^{(0)}$ ,  $\mathbf{a}_{i,j}^{(0)}$ 's and  $\mathbf{a}_{i,p+l}^{(0)}$ 's, we take the resulting minimisers as the initial values for  $\mathbf{b}_i^{(0)}$ ,  $\mathbf{a}_{i,j}^{(0)}$ 's and  $\mathbf{a}_{i,p+l}^{(0)}$ 's. Replacing  $\mathbf{b}_i^{(0)}$ ,  $\mathbf{a}_{i,j}^{(0)}$ 's and  $\mathbf{a}_{i,p+l}^{(0)}$ 's in (2.3) by their initial values and minimising (2.3) with respect to  $\mathbf{g}_{i,j}^{(0)}$ 's and  $\mathbf{g}_{i,p+l}^{(0)}$ 's, we take the resulting minimisers as the updated values for  $\mathbf{g}_{i,j}^{(0)}$ 's and  $\mathbf{g}_{i,p+l}^{(0)}$ 's. Continuing this iterative process until convergence, we get the minimiser of (2.3).

The minimisation of (2.5) is similar to that of (2.3). We start by choosing the initial values for  $\beta_k$ 's in (2.5) based on  $\tilde{\mathbf{g}}_{i,j}$ 's and  $\tilde{\mathbf{g}}_{i,p+l}$ 's obtained in Section 2.1.1. Specifically, the initial value for  $\beta_k$  is taken to be

$$\frac{1}{|\hat{\Delta}_k|} \sum_{(\iota,\ell) \in \hat{\Delta}_k} \tilde{\mathbf{g}}_{\iota,\ell}.$$

We replace  $\beta_k$ 's in (2.5) by their initial values, then minimise (2.5) with respect to  $\mathbf{b}$  and  $\alpha_k$ 's. We take the resulting minimisers as the initial values for  $\mathbf{b}$  and  $\alpha_k$ 's and substitute them for  $\mathbf{b}$  and  $\alpha_k$ 's in (2.5), then minimise (2.5) with respect to  $\beta_k$ 's. We take the resulting minimisers as the updated values for  $\beta_k$ 's, and continue this iterative process until convergence to get the minimiser of (2.5).

### 2.3 A couple of remarks

**Remark 1.** *The estimation of the partition in Section 2.1.2 can be further improved. Taking  $\{\hat{\Delta}_1, \dots, \hat{\Delta}_{\hat{m}}\}$  as an example, we can apply the following iterative process to improve the estimation:*

(1) *Compute*

$$\bar{g}_k(\cdot) = \frac{1}{|\hat{\Delta}_k|} \sum_{(i,j) \in \hat{\Delta}_k} \tilde{g}_{i,j}(\cdot), \quad k = 1, \dots, \hat{m},$$

where  $|\hat{\Delta}_k|$  is the cardinality of  $\hat{\Delta}_k$ .

(2) *For each  $(i, j) \in \mathcal{S}$ , we compute*

$$c_k = \int_0^1 \{\bar{g}_k(v) - \tilde{g}_{i,j}(v)\}^2 dv, \quad k = 1, \dots, \hat{m}.$$

*If  $c_{k_0}$  is the smallest  $c_k$ , then  $(i, j)$  belongs to set  $\hat{\Delta}_{k_0}^{(1)}$ . This leads to a partition  $\{\hat{\Delta}_1^{(1)}, \dots, \hat{\Delta}_{\hat{m}}^{(1)}\}$  of  $\mathcal{S}$ .*

(3) *We treat  $\{\hat{\Delta}_1^{(1)}, \dots, \hat{\Delta}_{\hat{m}}^{(1)}\}$  as  $\{\hat{\Delta}_1, \dots, \hat{\Delta}_{\hat{m}}\}$ , and repeat (1) and (2). Continuously doing so until convergence, we get an improved estimator of the partition  $\{\Delta_1, \dots, \Delta_m\}$ .*

**Remark 2.** *In the final estimation, an iterative process can be used to further improve the final estimators. Specifically, we substitute the minimiser of (2.5) for  $\tilde{\mathbf{b}}$ ,  $\tilde{\alpha}_k$ s and  $\tilde{\beta}_k$ s in (2.4), and minimise (2.4). We treat the resulting minimiser as updated  $\hat{\sigma}_\eta^2$  and  $\hat{\sigma}^2$ , and substitute them for the  $\hat{\sigma}_\eta^2$  and  $\hat{\sigma}^2$  in (2.5), then minimise (2.5) and substitute the resulting minimiser for  $\tilde{\mathbf{b}}$ ,  $\tilde{\alpha}_k$ s and  $\tilde{\beta}_k$ s in (2.4), and minimise (2.4) to get updated  $\hat{\sigma}_\eta^2$  and  $\hat{\sigma}^2$ . Continue this iterative process until convergence, and substitute the converged  $\hat{\sigma}_\eta^2$  and  $\hat{\sigma}^2$  for the  $\hat{\sigma}_\eta^2$  and  $\hat{\sigma}^2$  in (2.5), then minimise (2.5) to get the final  $\hat{\mathbf{b}}$ ,  $\hat{\alpha}_k$ s and  $\hat{\beta}_k$ s based on which improved final estimators of  $b(\cdot)$ ,  $a_{i,j}(\cdot)$ ,  $g_{i,j}(\cdot)$ ,  $a_{i,p+l}(\cdot)$ , and  $g_{i,p+l}(\cdot)$  are obtained.*

## 2.4 Selecting the values of the tuning parameters

In this section, we address several practical problems regarding the selection of the values of the tuning parameters in the proposed methods.

### 2.4.1 Selecting the optimal number of knots in the spline decomposition

Following the lead of [Hu et al. \(2019\)](#), we select the number of knots  $K_0$  via a Bayesian information criterion (BIC) approach:

$$\text{BIC}(K_0) = \log(\text{RSS}) + \mathcal{N} \frac{\log T}{T}.$$

The residual sum of squares (RSS) is defined in [\(2.3\)](#), which reflects the goodness of fit. Here,  $\mathcal{N} = (2p + 2q + 1)K_0$  controls the complexity of the model, and we assume  $T_i = T$  for the sake of clarification. The optimal number of knots  $K_0$  can be estimated by minimising the above BIC. According to [Theorem 1](#), it is reasonable to choose the optimal number of knots  $K_0$  on the interval  $[0.5T^{1/5}, 2T^{1/5}]$ , where  $\lfloor a \rfloor$  denotes the largest integer not larger than  $a$ . The number of knots  $K$  in the final estimation can be selected using the same approach.

### 2.4.2 Selecting the threshold $\mathcal{C}$ in the structure identification

The structure identification method relies on prior information about the threshold  $\mathcal{C}$ . However, it is usually unknown in practical applications and needs to be determined via a data-driven method. Actually, selecting  $\mathcal{C}$  is equivalent to selecting  $\hat{H}$  and  $\hat{m}$ . In this paper, following the lead of [Lian et al. \(2021\)](#), we can also apply the cross-validation method to select the two tuning parameters,  $\hat{H}$  and  $\hat{m}$ .

In particular, we implement a  $V$ -fold cross-validation approach. For a given pair  $\{H, m\}$ ,

we remove the  $1/V$ th member of the observed time points for

$$\{(y_{i,t}, u_{i,t}, \mathbf{X}_{i,t}), i = 1, \dots, n, t = 1, \dots, T_i\}$$

as a validation set. We estimate the semiparametric model (1.3) with identified structure on the remaining data, compute the squared error between  $y_{i,t}$  and the fitted values on the validation set, and repeat this procedure  $V$  times to calculate the cross-validated mean squared error. The optimal  $\hat{H}$  and  $\hat{m}$  can be estimated by minimising the cross-validation mean squared error.

### 3 Asymptotic theory

In this section, we are going to demonstrate the advantage of the proposed methodology by asymptotic theory. We will consider three different approaches:

- *Over-fitting*: Treat all unknown functions in model (1.3) as different functions to estimate. Namely, directly apply the final estimation described in Section 2.1.3 under the assumption that either of the two partitions involved is  $\{(i, j) : i = 1, \dots, n; j = 1, \dots, p + q\}$ .
- *Under-fitting*: Directly apply the final estimation to estimate the unknown functions under the assumption

$$a_{1,j}(\cdot) = \dots = a_{n,j}(\cdot), \quad g_{1,j}(\cdot) = \dots = g_{n,j}(\cdot),$$

for  $j = 1, \dots, p + q$ .

- *Correct fitting*: The proposed estimation is used to estimate the unknown functions.

In this section, we assume  $T_i \rightarrow \infty$ ,  $n$  possibly diverges to infinity, but  $H$  and  $m$  are fixed. This agrees with many real applications where  $H$  and  $m$  are expected to be small, and thus, there is a significant reduction of the unknown functions by clustering similar functions.

To keep the presentation concise, we state the asymptotic theorems in this section and leave all technical proofs in the supplementary material. Let

$$\mathbf{B}^{(0)}(u) = \left( B_1^{(0)}(u), \dots, B_{K_0}^{(0)}(u) \right)^\tau,$$

$$\mathbf{B}_i^{(0)}(u) = \left( B_1^{(0)}(u) - \bar{B}_{i,u,1}^{(0)}, \dots, B_{K_0}^{(0)}(u) - \bar{B}_{i,u,K_0}^{(0)} \right)^\tau,$$

$$\mathbf{B}_{i,j}^{(0)}(x) = \left( B_1^{(0)}(x) - \bar{B}_{i,x,j,1}^{(0)}, \dots, B_{K_0}^{(0)}(x) - \bar{B}_{i,x,j,K_0}^{(0)} \right)^\tau,$$

$$\tilde{\mathbf{A}}_{i,j}(u) = (\mathbf{0}^\tau, \dots, \mathbf{B}_i^{(0)\tau}(u), \dots, \mathbf{0}^\tau)^\tau, \quad \tilde{\mathbf{G}}_{i,j}(x) = (\mathbf{0}^\tau, \dots, \mathbf{B}_{i,j}^{(0)\tau}(x), \dots, \mathbf{0}^\tau)^\tau.$$

$\tilde{\mathbf{A}}_{i,j}(u)$  is a  $\{(p+q+1)K_0\}$ -dimensional vector consisting of  $(p+q+1)$  blocks of length  $K_0$ , with the  $(j+1)$ th block being  $\mathbf{B}_i^{(0)\tau}(u)$ , others all being  $\mathbf{0}$ .  $\tilde{\mathbf{G}}_{i,j}(x)$  is a  $\{(p+q)K_0\}$ -dimensional vector consisting of  $(p+q)$  blocks of length  $K_0$ , with the  $j$ th block being  $\mathbf{B}_{i,j}^{(0)\tau}(x)$ , others all being  $\mathbf{0}$ .

**Theorem 1** (Over-fitting case). *For any  $i$ ,  $i = 1, \dots, n$ , and  $1 \leq j \leq p+q$ , under the technical conditions (C1)–(C3) and (C5) in the supplementary material, if  $K_0 = O(T_i^{1/5})$ , we have*

$$T_i^{2/5} \left( \hat{b}(u) - b(u) - r(u) \right) \xrightarrow{D} N \left( 0, \tilde{\mathbf{A}}_{i,0}^\tau(u) \tilde{\Xi}_1^{-1} \tilde{\Sigma}_1 \tilde{\Xi}_1^{-1} \tilde{\mathbf{A}}_{i,0}(u) \right),$$

$$T_i^{2/5} \left( \hat{a}_{i,j}(u) - a_{i,j}(u) - r_{i,j}(u) \right) \xrightarrow{D} N \left( 0, \tilde{\mathbf{A}}_{i,j}^\tau(u) \tilde{\Xi}_1^{-1} \tilde{\Sigma}_1 \tilde{\Xi}_1^{-1} \tilde{\mathbf{A}}_{i,j}(u) \right),$$

$$T_i^{2/5} \left( \hat{g}_{i,j}(x) - g_{i,j}(x) - d_{i,j}(x) \right) \xrightarrow{D} N \left( 0, \tilde{\mathbf{G}}_{i,j}^\tau(x) \tilde{\Xi}_2^{-1} \tilde{\Sigma}_2 \tilde{\Xi}_2^{-1} \tilde{\mathbf{G}}_{i,j}(x) \right),$$

where  $\hat{b}(u)$ ,  $\hat{a}_{i,j}(u)$  and  $\hat{g}_{i,j}(x)$  are obtained by overfitting, the bias terms  $r(u) = b(u) - \mathbf{B}^{(0)\tau}(u)\mathbf{b}_i^{(0)}$ ,  $r_{i,j}(u) = a_{i,j}(u) - \mathbf{B}_i^{(0)\tau}(u)\mathbf{a}_{i,j}^{(0)}$ ,  $d_{i,j}(x) = g_{i,j}(x) - \mathbf{B}_{i,j}^{(0)\tau}(x)\mathbf{g}_{i,j}^{(0)}$  are of order  $O(K_0^{-2})$ .  $\tilde{\Xi}_1$  and  $\tilde{\Xi}_2$  are defined in condition (C5).  $\tilde{\Sigma}_1 = (\sigma^2 + \sigma_\eta^2) \int_0^1 \mathbb{E} \left[ \tilde{\mathbf{D}}_i(u) \tilde{\mathbf{D}}_i^\tau(u) \right] du$ ,  $\tilde{\Sigma}_2 = (\sigma^2 + \sigma_\eta^2) \int_0^1 \mathbb{E} \left[ \tilde{\mathbf{Z}}_i(x) \tilde{\mathbf{Z}}_i^\tau(x) \right] dx$ , and

$$\tilde{\mathbf{D}}_i(u) = \left( \mathbf{B}^{(0)\tau}(u), g_{i,1}(x_{i,t,1})\mathbf{B}_i^{(0)\tau}(u), \dots, g_{i,p+q}(x_{i,t,p+q})\mathbf{B}_i^{(0)\tau}(u) \right)^\tau,$$

$$\tilde{\mathbf{Z}}_i(x) = \left( a_{i,1}(u_{i,t})\mathbf{B}_{i,1}^{(0)\tau}(x), \dots, a_{i,p+q}(u_{i,t})\mathbf{B}_{i,p+q}^{(0)\tau}(x) \right)^\tau.$$

From Theorem 1, it is easy to see that the convergence rate of the estimators  $\hat{b}(u)$ ,  $\hat{a}_{i,j}(u)$  and  $\hat{g}_{i,j}(x)$  are of order  $T_i^{-2/5}$ , which is as expected, as we assume that the functions are twice differentiable.

**Theorem 2** (Under-fitting case). *Suppose the functions  $a_{i,j}(\cdot)$ s are sufficiently separated, i.e.,*

$$\frac{1}{n} \sum_{i=1}^n \int_0^1 \{a_{i,j}(u) - \bar{a}_1(u)\}^2 du > C > 0, \quad \bar{a}_1(u) = \frac{1}{n} \sum_{i=1}^n a_{i,j}(u),$$

then we have

$$\|\hat{a}_{i,j} - a_{i,j}\|_2 > C.$$

Similarly, we have

$$\|\hat{b} - b\|_2 > C, \quad \|\hat{g}_{i,j} - g_{i,j}\|_2 > C,$$

where  $\hat{b}(u)$ ,  $\hat{a}_{i,j}(u)$  and  $\hat{g}_{i,j}(x)$  are obtained by underfitting.

Theorem 2 shows that the estimators obtained by underfitting are not consistent. Before presenting Theorem 3, we introduce some notations: let

$$\mathbf{B}(u) = (B_1(u), \dots, B_K(u))^\tau, \quad \mathbf{B}_i(u) = (B_1(u) - \bar{B}_{i,u,1}, \dots, B_K(u) - \bar{B}_{i,u,K})^\tau,$$



$$\mathbf{B}_{i,j}(x) = (B_1(x) - \bar{B}_{i,x,j,1}, \dots, B_K(x) - \bar{B}_{i,x,j,K})^\tau,$$

$$\mathbf{A}_{i,j}(u) = (\mathbf{0}^\tau, \dots, \mathbf{B}_i^\tau(u), \dots, \mathbf{0}^\tau)^\tau, \quad \mathbf{G}_{i,j}(x) = (\mathbf{0}^\tau, \dots, \mathbf{B}_{i,j}^\tau(x), \dots, \mathbf{0}^\tau)^\tau.$$

$\mathbf{A}_{i,j}(u)$  is a  $\{(p+q+1)K\}$ -vector consisting of  $(p+q+1)$  blocks of length  $K$ , with the  $(j+1)$ th block being  $\mathbf{B}_i^\tau(u)$ , others all being  $\mathbf{0}$ .  $\mathbf{G}_{i,j}(x)$  is a  $\{(p+q)K\}$ -vector consisting of  $(p+q)$  blocks of length  $K$ , with the  $j$ th block being  $\mathbf{B}_{i,j}^\tau(x)$ , others all being  $\mathbf{0}$ .

**Theorem 3** (Correct fitting case). *Under the technical conditions (C1)–(C5) in the supplementary material, let  $N = \sum_{i=1}^n T_i$ . When  $K_0 = O(T_i^{1/5})$  and  $K = O(N^{1/5})$ , we have*

$$N^{2/5} \left( \hat{b}(u) - b(u) - r(u) \right) \xrightarrow{D} N \left( 0, \mathbf{A}_{i,0}^\tau(u) \Xi_1^{-1} \Sigma_1 \Xi_1^{-1} \mathbf{A}_{i,0}(u) \right),$$

$$N^{2/5} \left( \hat{a}_{i,j}(u) - a_{i,j}(u) - r_{i,j}(u) \right) \xrightarrow{D} N \left( 0, \mathbf{A}_{i,j}^\tau(u) \Xi_1^{-1} \Sigma_1 \Xi_1^{-1} \mathbf{A}_{i,j}(u) \right),$$

$$N^{2/5} \left( \hat{g}_{i,j}(x) - g_{i,j}(x) - d_{i,j}(x) \right) \xrightarrow{D} N \left( 0, \mathbf{G}_{i,j}^\tau(x) \Xi_2^{-1} \Sigma_2 \Xi_2^{-1} \mathbf{G}_{i,j}(x) \right),$$

where  $\hat{b}(u)$ ,  $\hat{a}_{i,j}(u)$  and  $\hat{g}_{i,j}(x)$  are obtained by correct fitting, and the bias terms  $r(u)$ ,  $r_{i,j}(u)$ ,  $d_{i,j}(x)$  are defined as Theorem 1 with order of  $K^{-2}$ .  $\Xi_1$  and  $\Xi_2$  are defined in condition (C5), and

$$\Sigma_1 = (\sigma^2 + \sigma_\eta^2) \int_0^1 \mathbb{E} [\mathbf{D}_k(u) \mathbf{D}_k(u)^\tau] du, \quad \Sigma_2 = (\sigma^2 + \sigma_\eta^2) \int_0^1 \mathbb{E} [\mathbf{Z}_k(x) \mathbf{Z}_k(x)^\tau] dx,$$

$$\mathbf{D}_k(u) = (\mathbf{B}^\tau(u), \beta_k(x_{i,t,1}) \mathbf{B}_i^\tau(u), \dots, \beta_k(x_{i,t,p+q}) \mathbf{B}_i^\tau(u))^\tau, \text{ if } (i,j) \in \mathcal{D}_k,$$

$$\mathbf{Z}_k(x) = (\alpha_k(u_{i,t}) \mathbf{B}_{i,1}^\tau(x), \dots, \alpha_k(u_{i,t}) \mathbf{B}_{i,p+q}^\tau(x))^\tau, \text{ if } (i,j) \in \Delta_k.$$

Theorem 3 shows that the convergence rates of the estimators  $\hat{b}(u)$ ,  $\hat{a}_{i,j}(u)$  and  $\hat{g}_{i,j}(x)$  are of order  $N^{-2/5}$ . This together with Theorem 1 shows that the estimators obtained by correct fitting have convergence rates with a higher order than those obtained by overfitting.

Therefore, they are more accurate.

Because the asymptotic variance of the above estimators has a very complicated form and it is not clear how to estimate it consistently, constructing a statistical inference based on the asymptotic normality established in Theorem 3 can be very challenging. In this paper, we do not consider the inference problem and leave it as an open question.

## 4 Simulations

In this section, we use a simulated example to demonstrate how well the proposed estimation procedure works and the risk of ignoring the homogeneity or heterogeneity among individuals.

In particular, the data are generated from the following semiparametric clustered data model:

$$y_{i,t} = b(u_{i,t}) + a_{i,1}(u_{i,t})g_{i,1}(y_{i,t-1}) + a_{i,2}(u_{i,t})g_{i,2}(x_{i,t}) + \eta_i + \epsilon_{i,t},$$

where  $u_{i,t}$  are generated from a uniform distribution  $U(0, 1)$ . The exogenous covariates are generated via a first-order autoregressive (AR) process with parameters  $\rho$  and  $\sigma$ , denoted by  $\text{AR}(1; \rho, \sigma)$ , which is given by  $x_{i,t} = \rho x_{i,t-1} + \sigma \zeta_{i,t}$ , where  $\zeta_{i,t}$  are generated from i.i.d. standard normal random variables. In particular,  $x_{i,t} \sim \text{AR}(1; 0.6, 0.5)$ , and  $\epsilon_{i,t}$  and  $\eta_i$  are independently generated from  $N(0, 0.1^2)$ .

The cluster-specific coefficient functions and additive functions are generated as follows:

$b(u) = 1.5 \cos(2\pi u)$ , and for each  $i = 1, 2, \dots, n$ ,

$$a_{i,1}(u) = \begin{cases} 1.3u \sin(2\pi u) + 1, & \text{when } i = 1, 2, \dots, n/2, \\ 1.3u \cos(2\pi u) + 1, & \text{when } i = n/2 + 1, \dots, n. \end{cases}$$



Figure 1: Toy example of the latent structures imposed on (a)  $a_{i,j}(\cdot)$  and (b)  $g_{i,j}(\cdot)$ .

$$a_{i,2}(u) = 2 \sin(1.5\pi u) - 1.2(u - 0.5)(1 - u) + 1,$$

and

$$g_{i,1}(y_{i,t-1}) = -0.8(1 - y_{i,t-1}^2)/(1 + y_{i,t-1}^2),$$

$$g_{i,2}(x_{i,t}) = \begin{cases} 2 \cos(\pi x_{i,t}/2) + 1.8 \sin(\pi x_{i,t}/3), & \text{when } i = 1, 2, \dots, n/2, \\ 1.5 \sin(\pi x_{i,t}/4) - 1.2 \cos(\pi x_{i,t}/3), & \text{when } i = n/2 + 1, \dots, n. \end{cases}$$

For the latent structure, Figure 1 describes a toy example of  $a_{i,j}(\cdot)$  and  $g_{i,j}(\cdot)$  ( $i = 1, \dots, n$  and  $j = 1, 2$ ), where different colours denote different functions.

We run the simulated example 100 times with various  $n$  and  $T$  and compare our proposed approach to its potential competitors based on the following performance metrics:

*Estimation accuracy.* For an estimator  $\hat{a}_{i,j}(\cdot)$  of  $a_{i,j}(\cdot)$ , its estimation accuracy can be evaluated based on the mean integrated squared error:

$$\text{MISE}(\hat{a}_{i,j}) = E \left\{ \int (\hat{a}_{i,j}(u) - a_{i,j}(u))^2 du \right\}.$$

To prevent the performance from being dominated by the poor boundary behaviour, we let

the integral domain be a non-boundary region, which is between the 1st and 99th quantiles of  $\{u_{it}\}$ .

*Consistency of the structure identification.* To evaluate the distance between the detected structure and the true one, we use the normalised mutual information (NMI) (Ke et al., 2016), which measures the similarity between two partitions. Suppose that  $\mathbb{C} = \{C_1, C_2, \dots\}$  and  $\mathbb{D} = \{D_1, D_2, \dots\}$  are two partitions of  $\{1, \dots, n\}$ , the NMI is defined as

$$\text{NMI}(\mathbb{C}, \mathbb{D}) = \frac{I(\mathbb{C}, \mathbb{D})}{[H(\mathbb{C}) + H(\mathbb{D})]/2},$$

where

$$I(\mathbb{C}, \mathbb{D}) = \sum_{k,j} (|C_k \cap D_j| / n) \log (n |C_k \cap D_j| / |C_k| |D_j|),$$

and

$$H(\mathbb{C}) = - \sum_k (|C_k| / n) \log (|C_k| / n).$$

The NMI takes values in  $[0, 1]$  with larger values indicating a higher level of similarity between the two partitions. For an estimated partition  $\hat{\mathcal{D}} = \{\mathcal{D}_1, \dots, \mathcal{D}_{\hat{H}}\}$  of  $\{(i, j) : 1, \dots, n, j = 1, \dots, p + q\}$ , obtained in stage 2 of the proposed estimation procedure in Section 2.1, we calculate  $\text{NMI}(\hat{\mathcal{D}}, \mathcal{D})$  to assess how close the true structure in  $a_{i,j}(\cdot)$  is to the estimated one. Similarly, we can calculate  $\text{NMI}(\hat{\Delta}, \Delta)$  to assess how close the true structure in  $g_{i,j}(\cdot)$  is to the estimated one.

The sample size  $T_i = 100, 200$  or  $400$  and  $n = 20$  or  $40$ . We estimate the unknown functions by overfitting, correct fitting and underfitting, respectively. The mean and standard deviation of NMI for the resulting estimators are presented in Table 1 and the mean squared errors of the resulting estimators are presented in Table 2.

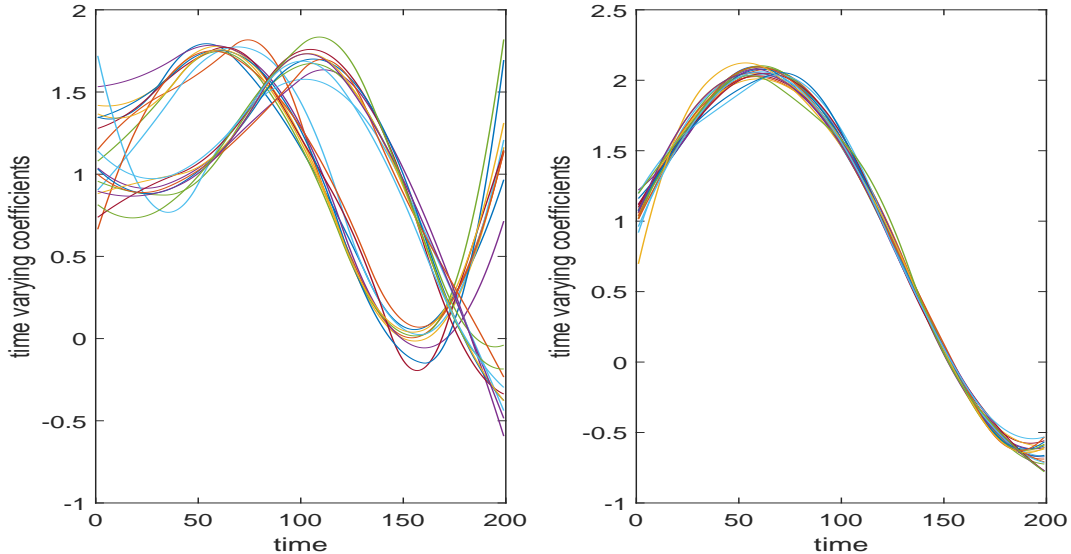


Figure 2: Median estimated varying-coefficient functions  $a_{i,j}(\cdot)$  based on 100 simulations when  $n = 20$  and  $T = 200$ . Left: Estimates of  $a_{i,1}(\cdot)$ . Right: Estimates of  $a_{i,2}(\cdot)$ .

## 4.1 Initial estimation

The initial estimates for subject-specific varying-coefficient functions  $a_{i,j}(\cdot)$  and additive functions  $g_{i,j}(\cdot)$  are presented in Figures 2 and 3. Note that the plotted median estimated functions correspond to the simulation which has the median MISEs. From these figures, we can see that the initial estimates for  $a_{i,1}(\cdot)$  and  $g_{i,2}(\cdot)$  have an obvious group structure, which is a preliminary validation of our simulation setup.

## 4.2 Structure identification

Based on the initial estimation, we can identify the latent structure using the procedure in Section 2.1.2. Note that in our simulation, the true partition for both  $a_{i,j}(\cdot)$  and  $g_{i,j}(\cdot)$  has three clusters (see Figures 2 and 3). Figures 4 and 5 present one simulation result of this step, which is aligned with our simulation setting. For example, in Figure 4, the left-hand side shows the initial estimates for  $a_{i,j}(\cdot)$ , the middle is the  $L_2$  distance matrix calculated based on  $a_{i,j}(\cdot)$  and the right-hand side is the result of the structure identification. The

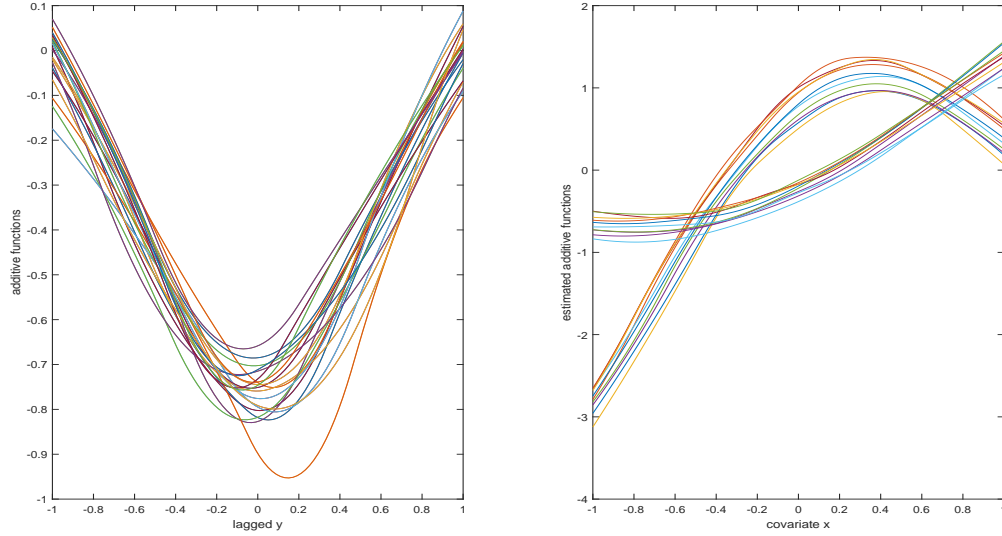


Figure 3: Median estimated additive functions  $g_{i,j}(\cdot)$  based on 100 simulations when  $n = 20$  and  $T = 200$ . Left: Estimates of  $g_{i,1}(\cdot)$ . Right: Estimates of  $g_{i,2}(\cdot)$ .

cluster membership is denoted by the colours.

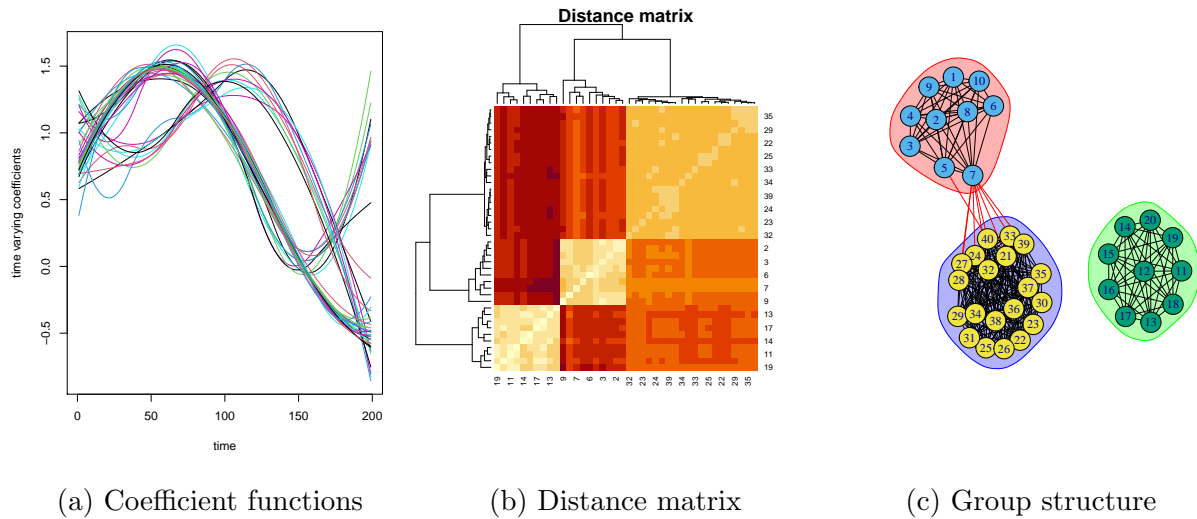


Figure 4: One typical run of structure identification for  $a_{i,j}(\cdot)$ , where  $i = 1, \dots, 20; j = 1, 2$ . (a) The estimates,  $\hat{a}_{i,j}(\cdot)$ , of specific coefficient functions for each subject  $i$ . (b) The distance matrix constructed by the  $L_2$  distance. (c) The identified structure, where the numbers  $(1, \dots, 40)$  denote the combinations of  $(i, j)$ .

The mean and standard deviation of the NMIs for  $a_{i,j}(\cdot)$  and  $g_{i,j}(\cdot)$  are shown in Table 1.

We can observe that as  $T$  gets larger, the performance becomes better. This makes sense

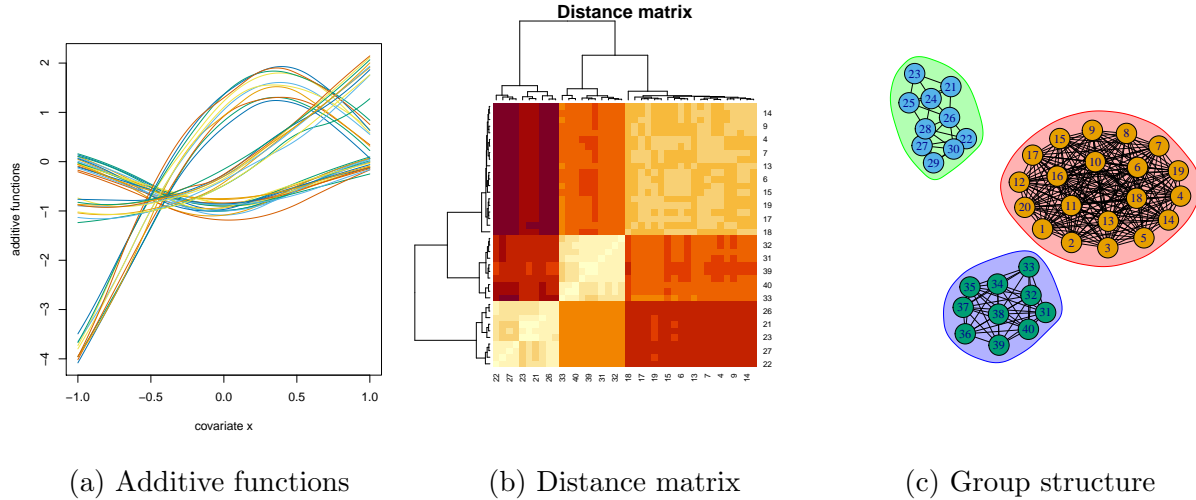


Figure 5: One typical run of structure identification for  $g_{i,j}(\cdot)$ . (a) The estimates,  $\hat{g}_{i,j}(\cdot)$ , of specific additive functions for each subject  $i$ . (b) The distance matrix constructed by the  $L_2$  distance. (c) The identified structure, where the numbers  $(1, \dots, 40)$  denote the combinations of  $(i, j)$ .

since the initial estimates improve as the sample size  $T$  increases.

Table 1: The mean and standard deviation of the NMIs for  $\mathcal{D}_H$  and  $\Delta_m$  based on 100 simulations with different sample size

|                 | $n/T$    | $T = 100$      | $T = 200$      | $T = 400$      |
|-----------------|----------|----------------|----------------|----------------|
| $\mathcal{D}_H$ | $n = 20$ | 0.8807(0.1406) | 0.9672(0.0596) | 0.9953(0.0296) |
|                 | $n = 40$ | 0.8755(0.1113) | 0.9720(0.0581) | 0.9948(0.0244) |
| $\Delta_m$      | $n = 20$ | 0.9669(0.0573) | 0.9920(0.0456) | 0.9987(0.0125) |
|                 | $n = 40$ | 0.8824(0.1198) | 0.9954(0.0181) | 0.9961(0.0170) |

### 4.3 Final estimation

We have illustrated the performance of the structure identification. We now assume that the true cluster structure is known in this step and adopt the procedure in Section 2.1.3 to estimate the cluster-specific functions. The final estimates are shown in Figures 6 and 7. In particular, we compare the estimation performance by plotting the final estimates and the true functions in the same figure. Obviously, the final estimates are all close to the true

functions.

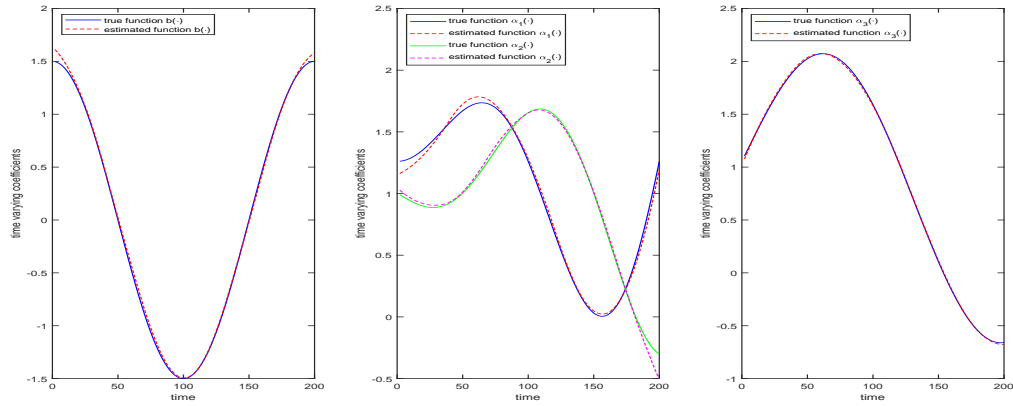


Figure 6: Median estimated varying-coefficient functions  $\alpha_k(\cdot)$  based on 100 simulations when  $n = 20, T = 200$ .

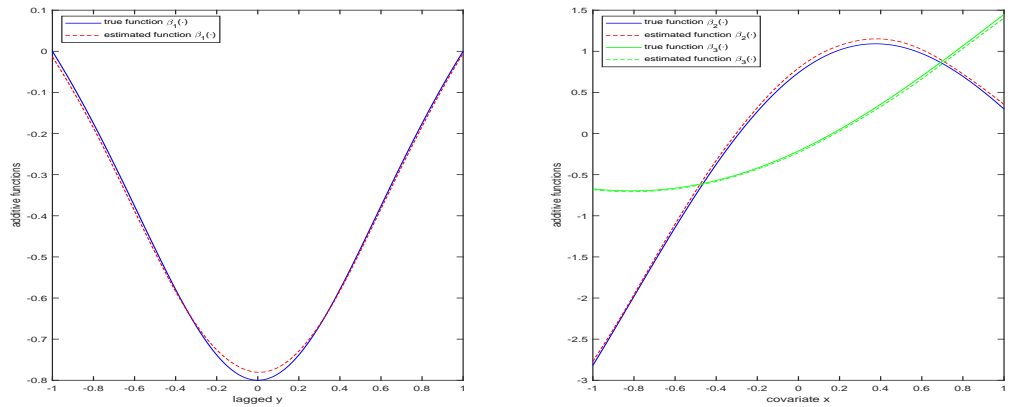


Figure 7: Median estimated additive functions  $\beta_k(\cdot)$  based on 100 simulations when  $n = 20, T = 200$ .

Finally, in Table 2, we compare the performance of correct fitting with overfitting and underfitting. We can observe that among these three methods, correct fitting provides the best performance with the lowest MISE. For correct fitting and overfitting, the overall estimation accuracy for all the unknown functions almost improves as  $T$  increases, which is somewhat expected, since as  $T$  increases, the initial estimates are better and the subsequent procedures rely more on the initial estimates. Note that the functions estimated by underfitting are not consistent, which agrees with Theorem 2.



Note that overfitting and underfitting, which either ignore or mistakenly specify the structure, perform worse than correct fitting, which illustrates the importance of incorporating the flexible and parsimonious structure in clustered data analysis.

Table 2: The mean and standard deviation of MISE for the estimated functions based on 100 simulations when  $n = 20$ .

| Function         | Method                 | $T = 100$      | $T = 200$      | $T = 400$      |
|------------------|------------------------|----------------|----------------|----------------|
| $b(\cdot)$       | <i>Correct fitting</i> | 0.0458(0.0144) | 0.0341(0.0141) | 0.0273(0.0113) |
|                  | <i>Overfitting</i>     | 0.1898(0.0220) | 0.1372(0.0194) | 0.1342(0.0186) |
|                  | <i>Underfitting</i>    | 0.1258(0.0177) | 0.1363(0.0146) | 0.1521(0.0192) |
| $a_{i,1}(\cdot)$ | <i>Correct fitting</i> | 0.0796(0.0234) | 0.0389(0.0093) | 0.0304(0.0064) |
|                  | <i>Overfitting</i>     | 0.2280(0.0523) | 0.1011(0.0109) | 0.0783(0.0143) |
|                  | <i>Underfitting</i>    | 0.3915(0.0097) | 0.3970(0.0062) | 0.4027(0.0099) |
| $a_{i,2}(\cdot)$ | <i>Correct fitting</i> | 0.0493(0.0090) | 0.0106(0.0025) | 0.0063(0.0017) |
|                  | <i>Overfitting</i>     | 0.1281(0.0196) | 0.0415(0.0038) | 0.0264(0.0024) |
|                  | <i>Underfitting</i>    | 0.1885(0.0071) | 0.0902(0.0041) | 0.0713(0.0108) |
| $g_{i,1}(\cdot)$ | <i>Correct fitting</i> | 0.0422(0.0102) | 0.0159(0.0048) | 0.0167(0.0039) |
|                  | <i>Overfitting</i>     | 0.1119(0.0121) | 0.0643(0.0047) | 0.0642(0.0051) |
|                  | <i>Underfitting</i>    | 0.1584(0.0136) | 0.2242(0.0153) | 0.3124(0.0197) |
| $g_{i,2}(\cdot)$ | <i>Correct fitting</i> | 0.0934(0.0068) | 0.0387(0.0033) | 0.0405(0.0013) |
|                  | <i>Overfitting</i>     | 0.2003(0.0161) | 0.1426(0.0024) | 0.0919(0.0016) |
|                  | <i>Underfitting</i>    | 0.5974(0.0008) | 0.6119(0.0006) | 0.6163(0.0008) |

## 5 Analysis of Covid-19 data from China

With the severity of the new coronavirus disease (Covid-19) outbreak, much literature focused on the prediction of growth trajectories, such as (Tang et al., 2021; Liu et al., 2021; Li and Linton, 2021, and references therein). Now we apply our method to analyse the Covid-19 data from a different perspective, mentioned in Section 1. For each day, we collected the cumulative number of confirmed cases ( $Z_{i,t}$ ), the number of people travelling from Wuhan to other provinces (<https://qianxi.baidu.com/>) and the maximum daily temperature (<http://www.weather.com.cn>).

The infection ratio is the response variable. It is denoted by  $y_{i,t}$  and is measured by  $\log(Z_{i,t}) - \log(Z_{i,t-1})$ .<sup>†</sup> To explore how the influential factors contribute to the infection ratio, we focus on first-order lagged dependent variable  $y_{i,t-1}$  and two covariates: (1) the proportion of the population of Wuhan travelling to the  $i$ th province on day  $t - 14$ , denoted by  $x_{i,t,1}$ ; (2) the maximum daily temperature in the  $i$ th province on day  $t$ , denoted by  $x_{i,t,2}$ . We first standardise  $y_{i,t-1}$  and the covariates  $x_{i,t,1}$  and  $x_{i,t,2}$  to  $[0, 1]$ , then apply the model (1.2), with  $p = 1$ ,  $u_{i,t} = t/T$ ,  $i = 1, \dots, 29$  and  $t = 1, \dots, 77$ , to fit the data. The proposed estimation procedure is implemented to estimate the unknown functions in the model.

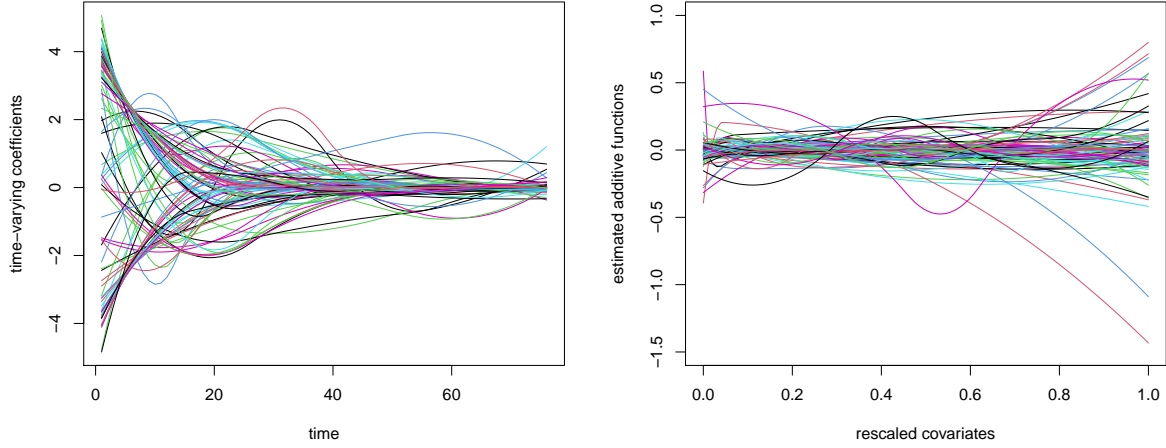
Specifically, we first apply the proposed method to estimate the province-specific coefficients, the obtained initial estimates of time-varying coefficients and additive functions are presented in Figure 8. We can see that both  $\hat{a}_{i,j}(\cdot)$  and  $\hat{g}_{i,j}(\cdot)$  have some homogeneous structures, which verifies the necessity of considering a latent structure model to characterise this homogeneity. A question naturally arises: How many clusters are there and which provinces share similar impacts?

In the structure identification step, we calculate the  $L_2$  distance between different functions, and identify the latent structure based on the proposed method in Section 2.1.2. The identified cluster memberships are presented in Tables 3 and 4. To save space, we put the visualization maps of these cluster memberships in the supplementary material.

For each identified cluster, we plot the initial estimates of time-varying coefficients or additive functions in that cluster, and present them in Figures 9 and 10. From Figures 9 and 10, we can roughly see that the coefficients  $\hat{a}_{i,j}(\cdot)$  and  $\hat{g}_{i,j}(\cdot)$  belonging to the same cluster have similar patterns, which illustrates that our proposed structure identification approach performs well.

---

<sup>†</sup>The time series plot of  $y_{i,t}$  for 29 provinces in China from 23 January to 8 April is presented in the supplementary material.



(a) Estimated time-varying coefficients  $\hat{a}_{i,j}(\cdot)$       (b) Estimated additive functions  $\hat{g}_{i,j}(\cdot)$

Figure 8: (a) Initial estimated time-varying coefficient functions  $\hat{a}_{i,j}(\cdot)$  for  $i = 1, \dots, 29; j = 1, 2, 3$ . (b) Initial estimated additive functions  $\hat{g}_{i,j}(\cdot)$  for  $i = 1, \dots, 29; j = 1, 2, 3$ .

Table 3: Identified cluster membership for time-varying coefficients  $\hat{a}_{i,j}(\cdot)$ .

| Cluster   | $\hat{a}_{i,1}(\cdot)$   | $\hat{a}_{i,2}(\cdot)$  | $\hat{a}_{i,3}(\cdot)$   |
|-----------|--|---|--|
| Cluster 1 | Anhui, Gansu, Guangdong, Guizhou, Henan, Jiangsu, Jiangsu, Jilin, Liaoning, Ningxia, Qinghai, Xinjiang, Yunnan | Anhui, Guizhou, Heilongjiang, Henan, Hunan, Jilin, Shanxi, Tianjin                      | Beijing, Chongqing, Gansu, Hainan, Heilongjiang, Hunan Inner mongolia, Jiangxi, Liaoning Qinghai, Shaanxi, Shanghai Shanxi, Sichuan, Tianjin, Yunnan, Zhejiang |
| Cluster 2 | Beijing, Fujian, Guangxi, Hainan, Hebei, Heilongjiang, Inner mongolia, Shanghai, Shanxi, Tianjin, Zhejiang     | Guangxi, Hainan, Inner mongolia, Jiangsu, Jiangxi, Ningxia, Shaanxi, Xinjiang, Zhejiang | Anhui, Fujian, Guangdong, Guangxi, Guizhou, Hebei, Jiangsu, Xinjiang   |
| Cluster 3 | Chongqing, Shaanxi, Sichuan  | Gansu, Guangdong, Liaoning  | Henan, Shandong  |
| Cluster 4 | Shandong   | Beijing, Chongqing, Fujian Hebei, Qinghai, Shandong Sichuan, Yunnan                     | Jilin, Ningxia   |
| Cluster 5 | Hunan  | -   | -  |
| Cluster 6 | -  | Shanghai  | -  |

Finally, based on the identified structure, we estimate  $b(\cdot)$ ,  $\alpha_k(\cdot)$  and  $\beta_k(\cdot)$  according to the procedure proposed in Section 2.1.3. The results are presented in Figure 11, where the left panel of Figure 11 denotes the estimated trend function. From the middle panel of Figure 11, we can conclude that the previous infection rate, maximum daily temperature

Table 4: Identified cluster membership for additive functions  $\hat{g}_{i,j}(\cdot)$ .

| Cluster   | $\hat{g}_{i,1}(\cdot)$   | $\hat{g}_{i,2}(\cdot)$   | $\hat{g}_{i,3}(\cdot)$  |
|-----------|--|--|---|
| Cluster 1 | Anhui, Chongqing, Fujian, Gansu, Guangxi, Guizhou, Hainan, Hebei, Heilongjiang, Inner mongolia, Jiangsu, Jiangxi, Jilin, Ningxia, Qinghai, Shaanxi, Shanghai, Sichuan, Tianjin, Xinjiang, Yunnan, Zhejiang | Fujian, Guangdong, Guangxi, Hebei, Hunan, Jiangxi, Jilin, Liaoning, Ningxia, Qinghai, Shanghai, Shanxi, Yunnan                   | Anhui, Beijing, Chongqing, Gansu, Guangdong, Hebei, Henan, Hunan, Inner mongolia, Jilin, Liaoning, Ningxia, Qinghai, Shandong, Shanghai, Shanxi, Sichuan, Tianjin, Xinjiang, Yunnan |
| Cluster 2 | Beijing, Guangdong, Henan, Hunan, Liaoning, Shandong, Shanxi   | Anhui, Beijing, Chongqing, Gansu, Guizhou, Hainan, Henan, Inner mongolia, Jiangsu, Shaanxi, Shandong, Sichuan, Tianjin, Zhejiang | Fujian, Guangxi, Hainan, Heilongjiang, Jiangsu, Jiangxi, Shaanxi, Zhejiang  |
| Cluster 3 | -  | Heilongjiang   | -   |
| Cluster 4 | -  | Xinjiang   | -   |
| Cluster 5 | -  | -  | Guizhou   |

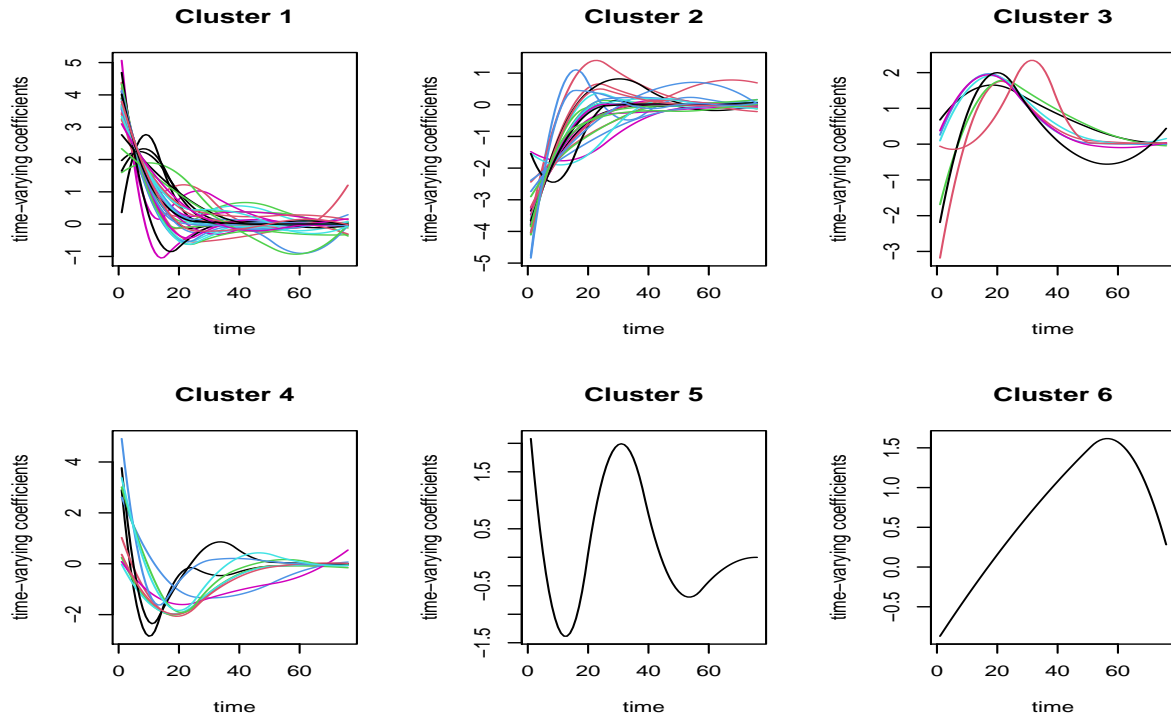


Figure 9: Identified latent structure for time varying coefficient functions  $\hat{a}_{i,j}(\cdot)$ , where  $i = 1, \dots, 29, j = 1, 2, 3$ .

and the number of people who travelled from Wuhan to the province have dynamic impacts on the infection ratio and the impacts vary over different provinces. The provinces which

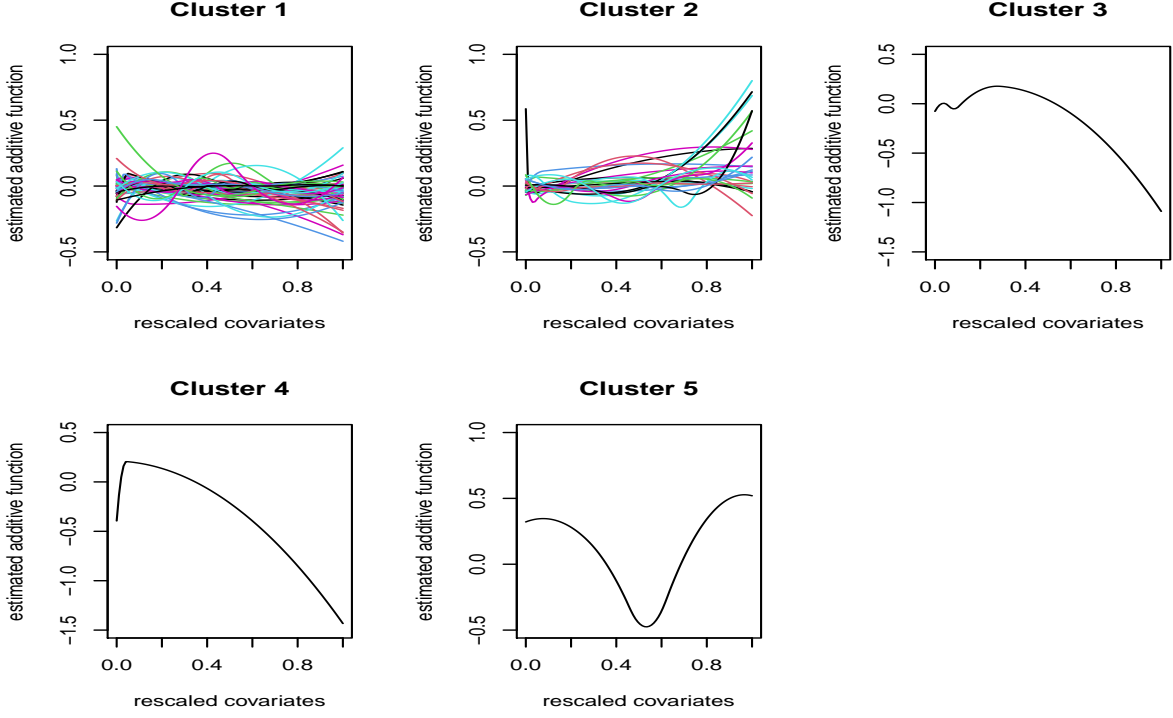


Figure 10: Identified latent structure for additive functions  $\hat{g}_{i,j}(\cdot)$ , where  $i = 1, \dots, 29, j = 1, 2, 3$ .

share the same impacts are depicted in Table 3. From the right panel of Figure 11, we can also find that the contribution of covariates to response is through transformed covariates and the contributions vary over different provinces. The cluster-specific functions and its corresponding functional changes are depicted in Table 5.

Furthermore, we examine the out of sample prediction performance between the proposed model (1.2) and the varying coefficient additive model (VCAM) without the lagged terms  $y_{i,t-1}$ . For a given fitted model, let  $e_{i,j} = (y_{i,T-j} - \hat{y}_{i,T-j})^2$  be the squared prediction error for the infection rate of the  $i$ th province on the  $(T - j)$ th day in the sample, based on the fitted model using all the observations before the  $(T - j)$ th day. Following Li et al. (2018) lead, we construct a cross-validation prediction error for the last 14 days as

$$PE = \frac{1}{14 \times 29} \sum_{i=1}^{29} \sum_{j=1}^{14} e_{i,j}.$$

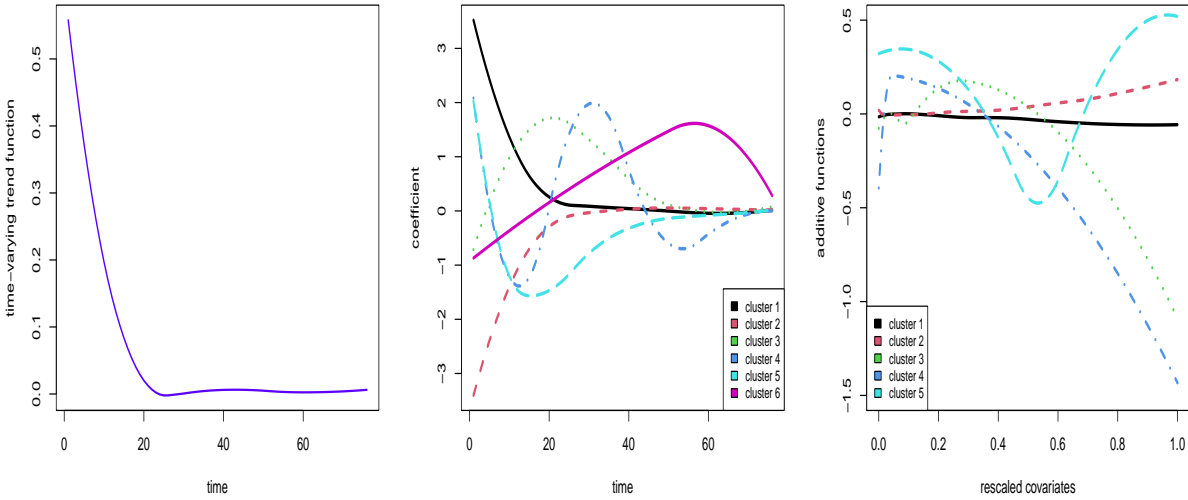


Figure 11: Final estimates of unknown functions. Left: estimated trend function  $b(\cdot)$ . Middle: estimated cluster-specific time-varying coefficient functions  $\alpha_k(\cdot), k = 1, \dots, 6$ . Right: estimated cluster-specific additive functions  $\beta_k(\cdot), k = 1, \dots, 5$ .

Table 5: Summary descriptions for the identified cluster-specific functions

| Function          | Cluster   | Cluster-specific function description  |
|-------------------|-----------|--|
| $b(\cdot)$        | Cluster 1 | The coefficients decreases from positive to zero gradually.                          |
| $\alpha_k(\cdot)$ | Cluster 1 | The coefficients decreases from positive to zero gradually.                          |
|                   | Cluster 2 | The coefficients increases from negative to zero gradually.                          |
|                   | Cluster 3 | The coefficients first increases from negative to positive, then decreases to zero.  |
|                   | Cluster 4 | The coefficients show a “W” shape.   |
|                   | Cluster 5 | The coefficients first decreases from positive to negative, then increases to zero.  |
|                   | Cluster 6 | The coefficients show an inverted “U” shape.   |
| $\beta_k(\cdot)$  | Cluster 1 | The function is a constant function with values zero.                                |
|                   | Cluster 2 | The function is a monotonic increasing function with positive values.                |
|                   | Cluster 3 | The function is a mixture of two quadratic functions.                                |
|                   | Cluster 4 | The function a monotonic decreasing function with negative values.                   |
|                   | Cluster 5 | The function is a quadratic function, the values first decreases and then increases. |

The PE for our proposed model (1.2) is 0.0053, and 0.0669 for VCAM, which verifies our proposed model is better than the VCAM in terms of out-of-sample prediction.

## 6 Concluding remarks

This paper has presented a flexible and parsimonious modelling mechanism for identifying and estimating latent structure in a class of semiparametric clustered data models in which the varying coefficients and additive functions are heterogeneous across clusters but homogeneous within a cluster and the cluster membership is unknown. In particular, we have considered identifying the hidden structure by a distance-based approach and estimating the cluster-specific functions with a three-stage method. We also established the asymptotic properties for the estimators obtained by overfitting, underfitting and correct fitting. The results of the simulations and an analysis of real data were provided to illustrate the finite-sample performance of the proposed method.

## References

- Bahadori, M. T., Kale, D., Fan, Y., and Liu, Y. (2015). Functional subspace clustering with application to time series. *ICML'15: Proceedings of the 32nd International Conference on Machine Learning*, 37:228–237.
- Bonhomme, S. and Manresa, E. (2015). Grouped patterns of heterogeneity in panel data. *Econometrica*, 83(3):1147–1184.
- Chen, J. (2019). Estimating latent group structure in time-varying coefficient panel data models. *The Econometrics Journal*, 22(3):223–240.
- Chen, Z., Fan, J., and Li, R. (2018). Error variance estimation in ultrahigh-dimensional additive models. *Journal of the American Statistical Association*, 113(521):315–327.

- Cheng, M.-Y. and Fan, J. (2016). Peter hall’s contributions to nonparametric function estimation and modeling. *Annals of Statistics*, 44(5):1837–1853.
- Cheng, M.-Y., Honda, T., and Zhang, J.-T. (2016). Forward variable selection for sparse ultra-high dimensional varying coefficient models. *Journal of the American Statistical Association*, 111(515):1209–1221.
- Chu, W., Li, R., Liu, J., and Reimherr, M. (2020). Feature selection for generalized varying coefficient mixed-effect models with application to obesity gwas. *Annals of Applied Statistics*, 14(1):276.
- Fan, A., Song, R., and Lu, W. (2017). Change-plane analysis for subgroup detection and sample size calculation. *Journal of the American Statistical Association*, 112(518):769–778.
- Fan, J., Fan, Y., Lv, J., and Yang, F. (2022). Simple-rc: Group network inference with non-sharp nulls and weak signals. *arXiv:2211.00128*.
- Feng, S., Li, G., Peng, H., and Tong, T. (2021). Varying coefficient panel data model with interactive fixed effects. *Statistica Sinica*, 31(2):935–957.
- Guo, C. and Li, J. (2022). Homogeneity and structure identification in semiparametric factor models. *Journal of Business and Economic Statistics*, 40(1):408–422.
- Hu, L., Huang, T., and You, J. (2019). Estimation and identification of a varying-coefficient additive model for locally stationary processes. *Journal of the American Statistical Association*, 114(527):1191–1204.
- Huang, J. Z. and Yang, L. (2004). Identification of non-linear additive autoregressive



- models. *Journal of the Royal Statistical Society: Series B (Statistical Methodology)*, 66(2):463–477.
- Kalli, M. and Griffin, J. E. (2018). Bayesian nonparametric vector autoregressive models. *Journal of Econometrics*, 203(2):267–282.
- Ke, Y., Li, J., and Zhang, W. (2016). Structure identification in panel data analysis. *Annals of Statistics*, 44(3):1193–1233.
- Ke, Y., Lian, H., and Zhang, W. (2022). High dimensional dynamic covariance matrices with homogeneous structure. *Journal of Business and Economic Statistics*, 40(1):96–110.
- Ke, Z. T., Fan, J., and Wu, Y. (2015). Homogeneity pursuit. *Journal of the American Statistical Association*, 110(509):175–194.
- Lei, H., Xia, Y., and Qin, X. (2016). Estimation of semivarying coefficient time series models with arma errors. *Annals of Statistics*, 44(4):1618–1660.
- Li, D., Ke, Y., and Zhang, W. (2015). Model selection and structure specification in ultra-high dimensional generalised semi-varying coefficient models. *Annals of Statistics*, 43(6):2676–2705.
- Li, G. and Li, W. (2008). Testing for threshold moving average with conditional heteroscedasticity. *Statistica Sinica*, 18(2):647–665.
- Li, G. and Li, W. (2011). Testing a linear time series model against its threshold extension. *Biometrika*, 98(1):243–250.
- Li, J., Huang, C., and Zhu, H. (2017). A functional varying-coefficient single-index model for functional response data. *Journal of the American Statistical Association*, 112(519):1169–1181.

- Li, J., Yue, M., and Zhang, W. (2019). Subgroup identification via homogeneity pursuit for dense longitudinal/spatial data. *Statistics in Medicine*, 38(17):3256–3271.
- Li, J., Zhang, W., and Kong, E. (2018). Factor models for asset returns based on transformed factors. *Journal of Econometrics*, 207(2):432–448.
- Li, S. and Linton, O. (2021). When will the covid-19 pandemic peak? *Journal of Econometrics*, 220(1):130–157.
- Lian, H., Qiao, X., and Zhang, W. (2021). Homogeneity pursuit in single index models based panel data analysis. *Journal of Business and Economic Statistics*, 39(2):386–401.
- Liu, J., Li, R., and Wu, R. (2014). Feature selection for varying coefficient models with ultrahigh-dimensional covariates. *Journal of the American Statistical Association*, 109(505):266–274.
- Liu, L., Moon, H. R., and Schorfheide, F. (2021). Panel forecasts of country-level covid-19 infections. *Journal of Econometrics*, 220(1):2–22.
- Pei, Y., Huang, T., Peng, H., and You, J. (2022). Network-based clustering for varying coefficient panel data models. *Journal of Business and Economic Statistics*, 40(2):578–594.
- Ren, Z., Kang, Y., Fan, Y., and Lv, J. (2019). Tuning-free heterogeneous inference in massive networks. *Journal of the American Statistical Association*, 114(528):1908–1925.
- Sang, P., Wang, L., and Cao, J. (2020). Estimation of sparse functional additive models with adaptive group lasso. *Statistica Sinica*, 30(3):1191–1211.
- Su, L., Shi, Z., and Phillips, P. C. (2016). Identifying latent structures in panel data. *Econometrica*, 84(6):2215–2264.

- Sun, Y. (2016). Functional-coefficient spatial autoregressive models with nonparametric spatial weights. *Journal of Econometrics*, 195(1):134–153.
- Sun, Y., Yan, H., Zhang, W., and Lu, Z. (2014). A semiparametric spatial dynamic model. *Annals of Statistics*, 42(2):700–727.
- Tang, F., Feng, Y., Chiheb, H., and Fan, J. (2021). The interplay of demographic variables and social distancing scores in deep prediction of us covid-19 cases. *Journal of the American Statistical Association*, 116(534):492–506.
- Vogt, M. and Linton, O. (2017). Classification of non-parametric regression functions in longitudinal data models. *Journal of the Royal Statistical Society: Series B (Statistical Methodology)*, 79(1):5–27.
- Wang, T. and Xia, Y. (2015). Whittle likelihood estimation of nonlinear autoregressive models with moving average residuals. *Journal of the American Statistical Association*, 110(511):1083–1099.
- Wood, S. N., Goude, Y., and Shaw, S. (2015). Generalized additive models for large data sets. *Journal of the Royal Statistical Society: Series C (Applied Statistics)*, 64(1):139–155.
- Wu, H., Fan, Y., and Lv, J. (2020). Statistical insights into deep neural network learning in subspace classification. *Stat*, 9(1):e273.
- Xiao, D., Ke, Y., and Li, R. (2021). Homogeneity structure learning in large-scale panel data with heavy-tailed errors. *Journal of Machine Learning Research*, 22(13):1–42.
- Xu, J., Yue, M., and Zhang, W. (2020). A new multilevel modelling approach for clustered survival data. *Econometric Theory*, 36(4):707–750.

- Yuan, M., Liu, R., Feng, Y., and Shang, Z. (2022). Testing community structure for hypergraphs. *Annals of Statistics*, 50(1):147–169.
- Zhang, W. and Lee, S.-Y. (2000). Variable bandwidth selection in varying-coefficient models. *Journal of Multivariate Analysis*, 74(1):116–134.
- Zhang, W., Lee, S.-Y., and Song, X. (2002). Local polynomial fitting in semivarying coefficient model. *Journal of Multivariate Analysis*, 82(1):166–188.
- Zhong, P.-S., Li, R., and Santo, S. (2019). Homogeneity tests of covariance matrices with high-dimensional longitudinal data. *Biometrika*, 106(3):619–634.
- Zhu, X., Xu, G., and Fan, J. (2022). Simultaneous estimation and group identification for network vector autoregressive model with heterogeneous nodes. *arXiv:2209.12229*.